Effect of Membrane Support Thickness on Supported Liquid Membrane Extraction of Levulinic Acid

Rajendaren, Vikneswary*[+]***; Saufi, Syed M.***
Department of Chemical Engineering, College of Engineering, Universiti Malaysia Pahang, Lebuhraya Tun Razak, 26300 Gambang, Pahang Darul Makmur, MALAYSIA

Zahari, M.A.K.M
Faculty of Chemical and Process Engineering Technology, Universiti Malaysia Pahang, Lebuhraya Tun Razak, 26300 Gambang, Pahang Darul Makmur, MALAYSIA

ABSTRACT: *One of the most appealing compounds in biomass products is levulinic acid (LA). At the same time, separating LA from biomass products is a significant issue in LA production. Supported liquid membrane (SLM) is a revolutionary technique for separating LA from biomass. This study studied the effect of different casting thicknesses of hybrid polyethersulfone graphene membrane from 300 µm to 450 µm on the membrane characteristic and extraction yield of LA via the SLM process. The liquid membrane impregnated into the membrane support was made of 0.3 M trioctylamine and 2-ethyl-1-hexanol. The morphology, surface contact angles, porosity, tensile strength, and performance of the support membrane were evaluated. The membrane cast at 400 µm extracted the most LA (86%) from the 10 g/L LA feed phase. It had an average porosity of 57.77%, surface contact angle at the top layer of 81.21°, surface contact angle at the bottom layer of 98.02°, and tensile strength of 8.41 N. The membrane casting thickness impacts the character of the membrane support and the overall performance of SLM. A suitable membrane structure is required to overcome the instability of the liquid membrane and increase the lifetime operation of SLM.*

KEYWORDS: *Supported liquid membrane; PES/graphene membrane; Casting thickness; Levulinic acid; Graphene.*

INTRODUCTION

Nowadays, the production of levulinic acid (LA) from biomass products is gaining significant attention from researchers to meet the world LA demand [1]. However, separating LA from other biomass products remains a substantial challenge in lowering the overall cost of LA production. Various methods were used to separate LA, such as adsorption [2], [3], electrodialysis [4], physical solvent extraction [5], distillation [6] and reactive extraction [7]. Most of these methods are high in cost, show inadequate efficiency, and can cause some negative

***** *To whom correspondence should be addressed.*
+ *E-mail: smsaufi@ump.edu.my*
1021-9986/2022/10/3725-3732 *8/$/5.08*

impacts to the environment [8]. SLM is a simple and efficient technique to remove and recover the desired product in a single step [9]. Hence, it can be an optimistic method for extracting and recovering LA from other products. A small amount of organic phase was used in SLM compare to conventional solvent extraction, thus reducing the separation cost [10–12].

Nevertheless, the loss of the organic liquid membrane phase from the membrane support is severe in SLM [13]. The support membrane acts as a phase boundary between the feed and removal phases and retains the organic liquid phase. The thickness of the membrane support has a significant impact on the liquid membrane's stability [14, 15]. SLM with a thick support membrane is more stable because it contains a more organic liquid phase. The thick organic phase restricted the formation of the water bridging between the feed and strip phases through the membrane pores [14]. Therefore, the organic phase is not easily ruptured or pushed out of the membrane pores. In contrast, a thin support membrane has the advantage of having a short solution diffusion pathway, which enhances the solute flux [15]. However, a thin membrane can quickly form a water bridge and wash out all the organic phases from the support membrane [14]. Furthermore, a thin membrane possesses low mechanical stability [16]. Thus it is easily ruptured at high pressure. Hence, there will be an optimum membrane thickness for the support membrane in the SLM.

Limited studies had been conducted on the effect of support membrane's properties on the SLM performance. Most of the SLM studies have used commercial membrane support. Thus, it is difficult to find suitable membrane support at various thicknesses to be tested in the SLM process. Commercial polypropylene membranes with different thicknesses of 25 µm, 100 µm, and 170 µm were used to extract model drugs in SLM by *Rysava et al.* [17]. The most efficient drugs transfers were obtained for the thinnest membrane of 25 µm. Although a relatively thin membrane may induce high SLM flux, it may easily lead to the organic liquid phase leakage from the membrane support [14]. For acetic acid removal, the Polyethersulfone (PES) membranes support was prepared at four different thicknesses between 300 µm to 400 µm by *Harruddin et al.* [18] for acetic acid removal. Based on their finding, the best acetic acid extraction was found at an optimum membrane thickness of 380 µm. SLM operated with the thinnest membrane support (300 µm) was not efficiently removes the acetic acid. Meanwhile, a thick support membrane can cause considerable solute accumulation in the organic phase and slow down the transport mechanism of the acetic acid in the SLM system [18].

Ideally, the membrane support in SLM should be porous and hydrophobic with proper tortuosity [19] to retain the organic liquid membrane inside the membrane support by capillary force [20]. Furthermore, the membrane support should have optimum pore length to achieve high SLM flux [15]. All these properties of the membrane support can be manipulated by adjusting the membrane casting thickness during the membrane fabrication step. The current study investigated the effect of different casting thicknesses from 300 µm to 450 µm on the structure and properties of hybrid PES/graphene membrane support. The membranes were characterized according to their hydrophobicity, porosity, and mechanical stability at different membrane thicknesses. LA extraction from aqueous solution through the SLM process was tested using different membrane support thicknesses. To the best of our knowledge, the properties of membrane support at different casting thickness and its performance in SLM process for LA separation has never been investigated so far.

EXPERIMENTAL SECTION

Materials

PES (Radel® A, Solvay, USA), graphene nanopowder (Low Dimensional Materials Research Centre, University of Malaya, Malaysia), polyethylene glycol, PEG 200 (Sigma Aldrich), and dimethylacetamide, DMaC (Sigma Aldrich) were mixed to form a dope solution for support membrane fabrication. The cast film was solidified in the tap water. The liquid membrane in the organic phase was formulated using 2-ethyl-1-hexanol (Sigma Aldrich), and trioctylamine, TOA (Sigma Aldrich). LA (Sigma Aldrich) and Sodium hydroxide, NaOH are the chemicals pumped at feed and stripping phases, respectively. Olive oil from Delima Oil Products Sdn. Bhd. was used to conduct the membrane porosity test.

Graphene/PES support membrane fabrication

The homogenous dope solution was prepared from 42.5 wt% PEG 200, 42.5 wt% DMaC 15 wt% PES, and an additional 0.1 wt% graphene nanopowder (%w/w of PES).

The membrane support was fabricated through the Vapor Induce Phase Separation (VIPS) technique, as previously reported [21]. The membranes were fabricated with different casting thicknesses of 300 µm, 350 µm, 400 µm, and 450 µm. The cast gel film was exposed to a humid environment at 86 % relative humidity for 30 seconds before being coagulated in a water bath at 40 °C for half an hour. After that, the solidified membrane was shifted to a room-temperature water bath for a one-day incubation to remove all excess solvents and chemicals on the membrane. The support membrane was allowed to dry at room temperature for two days to ensure the water is completely evaporated from the membranes.

Characterization of graphene/PES support membrane

Membrane Morphology

The membranes were frozen in nitrogen liquid and fractured by using forceps. The prepared samples were coated with platinum. The cross-sectional morphology of the membranes was observed by scanning electron microscope (SEM) ZEISS EVO 50.

Contact angle measurement

The contact angle of the membranes was determined to evaluate the hydrophobicity of the membranes. A microsyringe was used for dripping 5 µl of water on the membrane's surface. The contact angle between the membrane surface and the water droplet was measured using the optical contact angle measurement device (CAM 101 optical Contact Angle Meter, KSV Instruments). The average contact angle was obtained from three different membrane regions for each membrane sample.

Porosity measurement

In porosity measurement, the membranes prepared from different casting thicknesses were cut into a rectangular size of 10.5 cm × 4 cm and dried in a vacuum oven at 80℃ for 24 hours to remove the water from the support membranes altogether. The dried membranes were then weighted as W_1.

The membrane was then immersed in olive oil for one day to allow the oil to fill the pores and empty spaces in the support membrane. The filter paper was used to remove excess olive oil on the wet membrane surface. Next, the wet membrane was weighted and recorded as W_2. The three membrane samples average porosity was calculated. Eq. (1) was used to compute the membrane porosity, ε, (%).

$$\varepsilon = \frac{W_2 - W_1}{\rho V_1} \times 100\% \quad (1)$$

Where W_1 and W_2 are the dry and wet membrane weights (g), respectively. V_1 represents the membrane volume (cm^3). Moreover, the density of olive oil is 0.8 g/cm^3 and is represented by ρ in the equation.

Mechanical Strength

The support membranes were cut into a rectangular shape of 50 mm × 20 mm size. The membranes' tensile strength (N) was measured using Shimadzu EZ-LX Universal Testing Machine with a loading velocity of 5 mm/min. Three membrane samples were tested, and the average tensile strength was calculated.

Supported liquid membrane system

As previously illustrated in detail, the prepared SLM was placed between two Teflon compartment membrane cells and fitted into the SLM system [21]. The membrane support was incubated into an organic phase of 0.3 M TOA in 2-ethyl-1-hexanol for 24 hours. At a 50 mL/min flow rate, 10 g/L of LA aqueous solution and 0.5 M of NaOH solution were circulated in counter-current flow directions as the feed and strip phases, respectively. For eight hours, samples were obtained from the feed phase every two hours for examination.

LA extraction yield

The concentration of LA at the feed phase over time was determined using the Agilent high-performance liquid chromatography (HPLC) 1200. The column used to detect LA was the Synergy Hydro C18 HPLC column (Phenomenex, 250 mm × 4.6 mm, 4 µm particle size). In HPLC analysis, potassium dihydrogen phosphate with a molarity of 0.02 M and a pH of 2.9 was used as the mobile phase. The peak response was detected using an UltraViolet (UV) detector with a wavelength of 221 nm. Eq. 2 was used to calculate the percentage of LA extracts from the feed phase:

$$\text{LA extraction } (\%) = \frac{[\text{LA}]_{\text{fi}} - [\text{LA}]_{\text{fo}}}{[\text{LA}]_{\text{fi}}} \times 100\% \quad (2)$$

Where $[LA]_{fi}$ and $[LA]_{fo}$ indicate the initial and final *LA* concentrations in the feed phase, respectively.

RESULTS AND DISCUSSION

Membrane characterization

Morphology of membrane support

The morphology of the PES/graphene support membranes prepared at different casting thicknesses is shown in Fig. 1. It was observed that the actual thickness of the membranes support was 35 to 43% smaller than the membrane casting thickness due to the effect of the surface tension acting on the dope solution before the membrane solidification and during the membrane drying process [22, 23]. The membrane cast at 300 µm, 350 µm, 400 µm, and 450 µm showed a final membrane thickness of 170 µm, 200 µm, 250 µm, and 290 µm, respectively.

An asymmetrical structure consisted of a thick, dense layer at the top, and a finger-like structure at the bottom was formed in a membrane cast at 300 µm. This structure can be correlated with the short diffusion distance experienced by the solvent during the phase inversion process. Solvent within the thin film can be diffused easily and rapidly from cast solution to form a thick, dense layer on top of the membrane [24]. Diffusion of non-solvent through the thick layer has created the pores below the thick layer, and the continuous diffusion of the non-solvent into the pores has caused growth in pores. The remaining solvent diffused into the growing pores, resulting in a polymer-rich phase around the pores. The pore stopped growing when the polymer-rich region's surroundings solidified utterly. Furthermore, the fusion of two poor – polymers at the bottom layer before wall solidification has formed larger pores at the bottom part of the membrane.

The membranes from casting thicknesses of 350 µm and 450 µm consist of thin, dense layers at the top of each membrane, as shown in Fig. 1. Moreover, the size of the finger-like structure in the membranes also increases from top to bottom layer due to the late wall solidification of polymer-rich that surrounds the pore at the bottom part of the membranes. Apart from that, membranes fabricated by a casting thickness of 400 µm form cylindrical microvoids from top to bottom of the membrane. The large diffusion distance has caused slower solvent diffusion from the casting solution and fast diffusion of non-solvent into the casting solution, thus forming a porous top layer. This porous structure at the top layer has only slightly affected the diffusion rate of the sublayer, promoting a similar phase transition across the membrane [25]. Hence, the formed microvoids are evenly distributed across the membrane's cross-section.

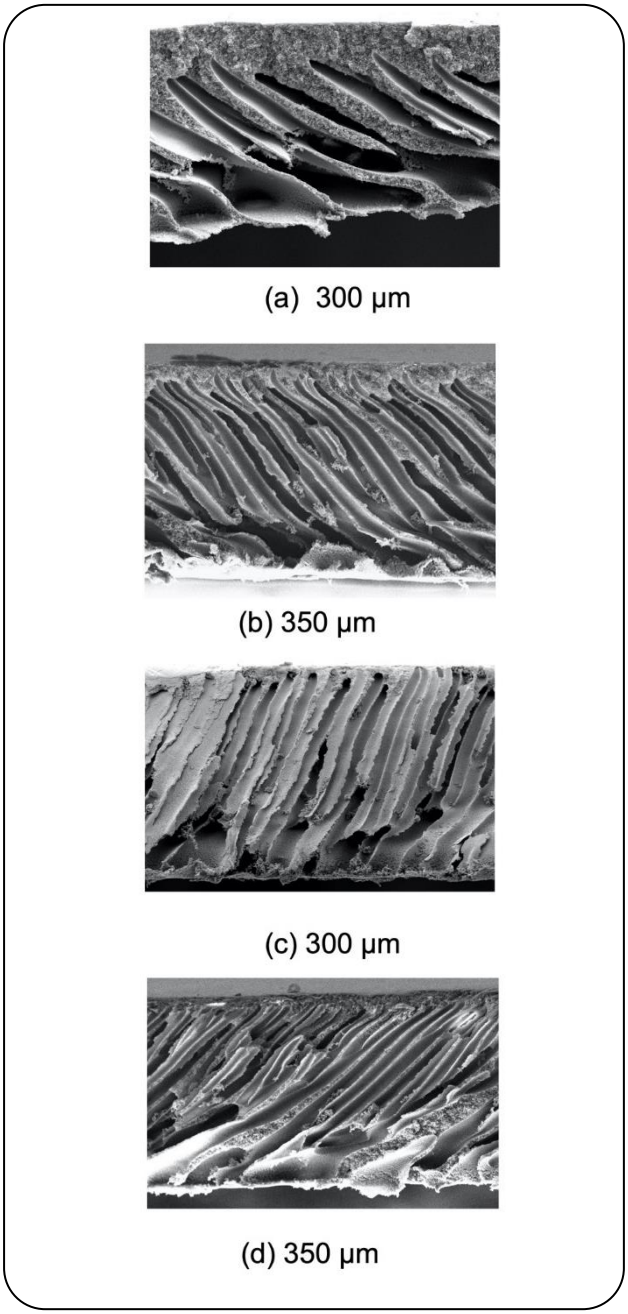

Fig. 1: Top to bottom. cross-section of flat sheet PES/graphene hybrid membranes by casting thickness at (a) 300 µm, (b) 350 µm, (c) 400 µm, and (d) 450 µm.

Even though 450 µm of cast film has a long diffusion distance, the lower concentration of the polymer at the top surface has resulted in a thin skin layer [26]. Moreover, the fast solvent diffusion at the top layer and slow solvent diffusion at the sublayer have reduced the precipitation rate at the sublayer. As a result, a membrane with a small dense layer followed by a porous sublayer was formed.

Contact angle

PES is a hydrophilic polymer with high surface energy. Meanwhile, graphene is a highly hydrophobic inorganic filler. The introduction of graphene nanopowder into the PES solution can modify the function of the hydrophilic group in the PES and change the membrane to having a highly hydrophobic character [21, 27]. The surface contact angles of the hybrid PES/graphene membrane cast at various thicknesses are shown in Fig. 2. Based on the literature review, the support membrane is classified as hydrophobic and superhydrophobic when the membrane contact angle is greater than 90° and 150°, respectively [27]. The average top surface contact angle for all membranes was less than 90° and considered hydrophilic. In contrast, the bottom surface of all membranes had contact angle values above 90°. This trend could be related to the distribution of graphene within the membrane matrix. Most of the graphenes were located at the bottom of the membrane and contributed to the contact angle enhancement in the bottom layer. The porous structure of the membrane also influences the contact angle value. In general, the surface of the bottom layers is more porous, possessing a higher contact angle than that at the top surface of the membranes [28]. The value of the contact angle varied between the membranes cast at different thicknesses due to the different porous structures of the membrane. The membrane prepared at 300 µm has a thick, dense top layer without any surface pores, showing the smallest contact angle of 73.40° for the top surface. However, it also had the highest contact angle (104.8°) for the bottom surface due to its porous surface. The membrane cast at 400 µm was considered the best membrane with a contact angle reading of 81.21° and 98.02° for the top and bottom surfaces, respectively. Even though the membrane's top layer was hydrophilic, the organic liquid membrane had remained stable during the SLM experiment without any leakage in the organic phase.

A membrane cast at 400 µm was considered the best membrane with contact angle values of 81.21° and 98.02° for the top and bottom layers, respectively.

Membrane Porosity

The porosity of the membranes prepared at different casting thicknesses is shown in Fig. 3. The porosity decreased as the membrane thicknesses increased due to the increase in the total membrane volume. Membrane

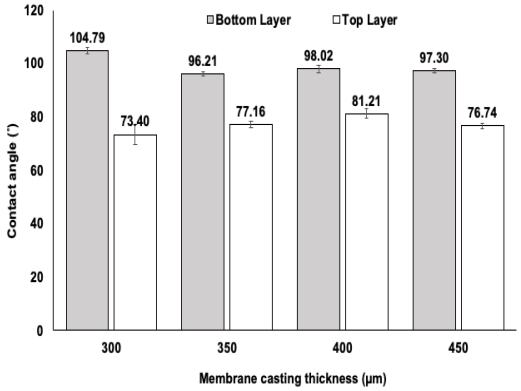

Fig. 2: Average contact angle readings for top and bottom surface layer of the membranes.

prepared at 300 µm and 450 µm had the highest porosity of 93.9% and lowest porosity of 75.4%, respectively. The number of pores, pore size, and tortuosity [29] also significantly affected the membrane porosity. The membrane prepared at 400 µm had higher porosity than the membrane of 350 µm thickness, although its membrane volume is bigger. The void volume of space inside the membrane structure can be represented by the volume of oil-impregnated in the membrane during the porosity measurement. The amount of oil-impregnated by the membrane with 400 µm and 350 µm thicknesses were 0.96 mL and 0.71 mL, respectively. By judging on oil volume impregnated, the membrane at 400 µm had a massive number of highly interconnected big-sized cylindrical micropores that contribute to the large void volume. Therefore, the porosity of the 400 µm membrane is high, although it had a higher membrane volume than the 350 µm membrane.

Mechanical Strength

The maximum amount of tensile stress that a material can endure before breaking is called tensile strength. The higher the tensile strength, the higher the resistance of the membrane to breaks under tension. Hence, a membrane with high tensile strength can remain stable in the SLM system without any breakage for an extended period. Fig. 4 shows the tensile strength of the membranes prepared at different thicknesses. The tensile strength increased from 4.64 N to 8.41N, as the casting thickness increased from 300 µm to up to 400 µm. However, the tensile strength was reduced when the casting thickness was further increased to 450 µm. Apart from that,

the mechanical strength of a membrane is also highly affected by the open support layer [30]. Based on the morphology of the membranes fabricated at 400 µm, an open support layer was formed, resulting in the highest mechanical strength at around 8.41 N.

Extraction of LA

The pore structure and porosity of the membranes play an essential role in SLM [15]. In this study, these properties of the membranes were modified by adjusting the casting thickness of the membranes. The extraction yield of LA by using different thicknesses of the support membrane is shown in Fig. 5. The highest LA extraction of 86% was achieved using the membrane that was cast at 400 µm thickness. This membrane showed the largest volume of space among the membrane reported, as discussed in the porosity section. It can accommodate a more liquid membrane phase within it. Moreover, the open support layer structure of the membrane had improved the transportation of LA from the feed to the stripping phase. Although the membrane at 300 µm had the highest porosity, it only had 0.67 ml void volume. Less amount of liquid membrane phase is contained in this membrane. In addition, it had a very thick top layer that can interrupt the interaction between the organic and stripping phase. Thus, it resulted in the lowest LA extraction of 78%. The membrane prepared at 350 µm had a shorter pore length and was thinner than the membrane prepared at 450 µm thickness. The shorter pore length transferred the solute-carrier complex more easily and rapidly to the stripping phase. Therefore, the membrane cast with 350 µm thickness showed a higher LA extraction than the membrane cast with 450 µm thickness.

CONCLUSIONS

The casting thickness of the membrane highly impacts the membrane's characteristics and LA extraction in the SLM process. An adequate membrane thickness prevents the formation of a water bridge that causes instability problems in the SLM process. At optimum membrane thickness, the loss of liquid membrane can be prevented, and the LA's separation from the feed phase can be enhanced. The PES/graphene membrane with 400-µm thickness had formed an open support layer with a finger-like porous structure across the membrane, showing the highest LA extraction yield of 86%. Moreover, this membrane had the highest tensile strength, surface contact angles for both layers, and the highest void space for liquid membrane impregnation. Hence, it is suitable to be employed in the SLM process as membrane support.

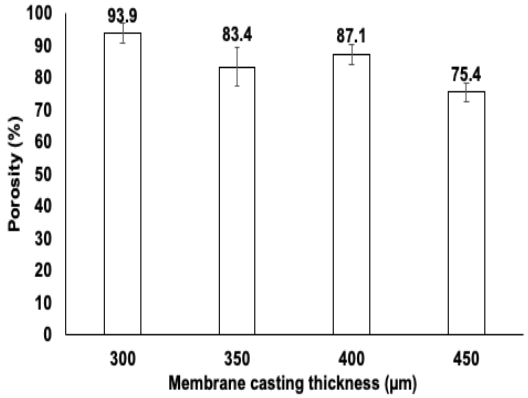

Fig. 3: Porosity (%) of the membranes.

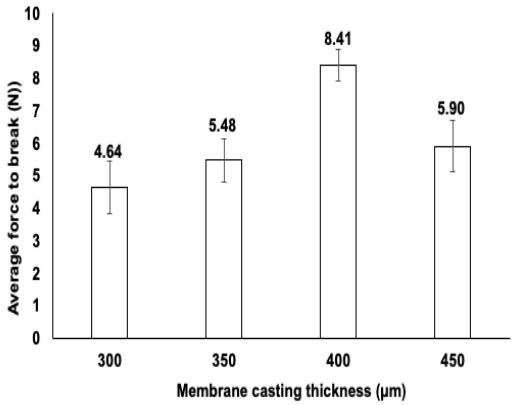

Fig. 4: Average force applies to the membranes to break.

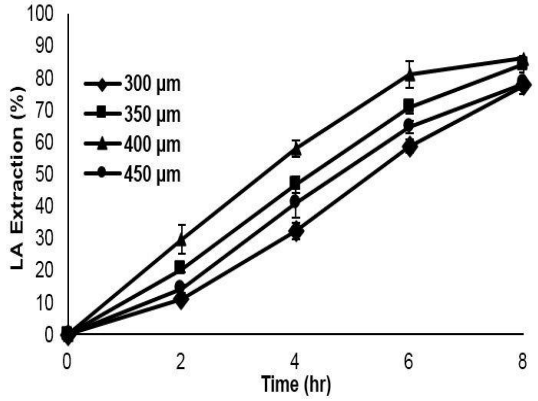

Fig. 5: Extraction yield of LA using membranes that fabricated from different casting thickness.

Acknowledgements

Vikneswary Rajendaren would like to express her gratitude to the Universiti Malaysia Pahang for sponsoring her Ph.D. study under UMP Doctoral Research Scheme (DRS) and UMP Post Graduate Research Scheme (PGRS1903114).

Received: Oct. 29, 2021 ; Accepted: Jan. 3, 2022

REFERENCES

[1] Girisuta B., "Levulinic Acid from Lignocellulosic Biomass," PhD Thesis. University of Groningen, (2007).

[2] Datta D., Uslu H., Adsorption of Levulinic Acid from Aqueous Solution by Amberlite XAD-4, *J. Mol. Liq.*, **234(C)**: 330–334 (2017).

[3] Liu B., Zeng L., Mao J., Ren Q., Simulation of Levulinic Acid Adsorption in Packed Beds Using Parallel Pore / Surface Diffusion Model, *Chem. Eng. Technol.*, **33(7)**: 1146–1152 (2010).

[4] Habe H., et al., Electrodialytic Separation of Levulinic Acid Catalytically Synthesized from Woody Biomass for Use in Microbial Conversion, *Biotechnol. Prog.*, **33(2)**: 448–453(2017).

[5] Mascal M., Nikitin E.B., High-Yield Conversion of Plant Biomass into the Key Value-Added Feedstocks 5- (Hydroxymethyl) Furfural , Levulinic Acid , and Levulinic Esters via 5- (Chloromethyl) Furfural, *Green Chem.*, **12**: 370–373(2010).

[6] Long N.V.D., Hong J., Nhien L.C., Lee M., Novel Hybrid-Blower-and-Evaporator-Assisted Distillation for Separation and Purification in Biorefineries, *Chem. Eng. Process. Process Intensif.*, **123**: 195–203 (2018).

[7] Kumar S., Uslu H., Datta D., Rarotra S., Rajput K., Investigation of Extraction of 4‑Oxopentanoic Acid by N,N‑Dioctyloctan-1-Amine in Six Different Diluents: Equilibrium Study, *J. Chem. Eng. Data*, **60(5)**: 1447–1453(2015).

[8] Tugtas A.E., Fermentative Organic Acid Production and Separation, *Fen Bilim. Derg.*, **23(2)**: 70–78 (2011).

[9] Rajendaren V., Saufi S.M., Zahari M.A.K., Mohammad A.W., Carrier Selection in Liquid Membrane for Extraction of Levulinic Acid Using Hybrid Graphene-Polyethersulfone Supported Liquid Membrane, *Mater. Today Proc.*, **17**: 1117–1125 (2019).

[10] Kislik V.S., "Introduction, General Description, Definitions, and Classification. Overview," *Liquid Membranes : Principles and Applications in Chemical Separations and Wastewater Treatment*, 1st ed., Elsevier B.V., Burlington (2010).

[11] López-Garzón C.S., Straathof A.J.J., Recovery of Carboxylic Acids Produced by Fermentation, *Biotechnol. Adv.*, **32(5)**: 873–904(2014).

[12] Rajendaren V., Saufi S.M., Zahari M.A.K., Mohammad A.W., Study on Stripping Phase Conditions on the Levulinic Acid Extraction Using Supported Liquid Membrane, *J. Mech. Eng. Sci.*, **13(3)**: 5625–5636(2019).

[13] Tripathi S., Anjum S., Liquid Membrane Is a Boom for Extraction / Removal of Substances, *J. Chem. Eng. Its Appl.*, **2(2)**: 20–36(2017).

[14] Kemperman A.J.B., Bargeman D., Boomgaard T.V. D., Strathmann H., Stability of Supported Liquid Membranes : State of the Art, *Sep. Sci. Technol.*, **31(20)**: 2733–2762(1996).

[15] Dzygiel P., Wieczorek P.P., "Supported Liquid Membranes and Their Modifications : Definition , Classification , Theory , Stability , Application and Perspectives", *Liquid Membranes: Principles and Applications in Chemical Separations and Wastewater Treatment*, 1st ed., P. Dzygiel and P. P. Wieczorek, Eds. Elsevier B.V, Poland (2010).

[16] Kools W.F.C., "Membrane Formation by Phase Inversion in Multicomponent Polymer Systems," PhD Thesis. University of Twente, (1998).

[17] Ryšavá L., Dvořák M., Kubáň P., The Effect of Membrane Thickness on Supported Liquid Membrane Extractions In-Line Coupled to Capillary Electrophoresis for Analyses of Complex Samples, *J. Chromatogr. A*, **1596**: 226–232 (2019).

[18] Harruddin N., Saufi S.M., Ku C., Faizal M., Wahab A., Removal of Acetic Acid from Aqueous Solution by Polyethersulfone Supported Liquid Membrane, *Chem. Eng. Trans.*, **56(2014)**: 847–852 (2017).

[19] Parhi P.K., Supported Liquid Membrane Principle and Its Practices: A Short Review, *J. Chem.*, **2013**: 1–11 (2013).

[20] Shimoyama Y., Neha T., Permeability and Separation Coefficient of Carbon Dioxide through Glycol Derivative Supported Liquid Membrane, *J. Memb. Sci.*, **469:** 300–305 (2014).

[21] Harruddin N., Saufi S.M., Faizal C.K.M., Mohammad A.W., Ming H.N., Supported Liquid Membrane Using Hybrid Polyethersulfone/ Graphene Flat Sheet Membrane for Acetic Acid Removal, *J. Phys. Sci.*, **28**: 111–120 (2017).

[22] Thakur S., Malviya P. K.S.R., Influence of Concentration on Surface Tension & Viscosity of Tamarind (Tamarindus Indica) Seed Gum, *Chemistry (Easton).*, **1(1)**: 008–012 (2017).

[23] Ramesh G., Narayan Prabhu K., Effect of Polymer Concentration on Wetting and Cooling Performance during Immersion Quenching, *Metall. Mater. Trans. B Process Metall. Mater. Process. Sci.*, **47(B)**: 859–881 (2016).

[24] Young T.H., Chen L.W., Pore Formation Mechanism of Membranes from Phase Inversion Process, *Desalination*, **103(3)**: 233–247 (1995).

[25] Gencal Y., Durmaz E.N., Culfaz-emecen P.Z., Preparation of Patterned Micro Filtration Membranes and Their Performance in Cross Flow Yeast Filtration, *J. Memb. Sci.*, **476**: 224–233 (2015).

[26] Shahmirzadia M.A.A., Hosseinia S.S., Ruan G., Tan N.R.,"Tailoring PES Nanofiltration Membranes through Systematic Investigations on the Effect of Prominent Design, Fabrication and Operational Parameters, *R. Soc. Chem.*, **5**: 49080–49097 (2015).

[27] Ahmad N.A., Leo C.P., Ahmad A.L., Ramli W.K.W., Membranes with Great Hydrophobicity: A Review on Preparation and Characterization, *Separation and Purification Reviews*, **44(2)**: 109–134 (2015).

[28] Rahimpour A., Madaeni S.S., Mansourpanah Y., Fabrication of Polyethersulfone (PES) Membranes with Nano-Porous Surface Using Potassium Perchlorate (KClO4) as an Additive in the Casting Solution, *Desalination*, **258(1–3)**: 79–86 (2010).

[29] Harruddin N., Saufi S.M., Faizal C.K.M., Mohammad A.W., Effect of VIPS Fabrication Parameters on the Removal of Acetic Acid by Supported Liquid Membrane Using a PES-Graphene Membrane Support, *RSC Adv.*, **8(45)**: 25396–25408(2018).

[30] Baker R.W., *Membrane Technology and Applications*. John Wiley & Sons Ltd (2012).